

Pneumatic Multi-mode Silicone Actuator with Pressure, Vibration, and Cold Thermal Feedback

Mohammad Shadman Hashem, Ahsan Raza, Sama E Shan, and Seokhee Jeon*

Abstract—A wide range of haptic feedback is crucial for achieving high realism and immersion in virtual environments. Therefore, a multi-modal haptic interface that provides various haptic signals simultaneously is highly beneficial. This paper introduces a novel silicone fingertip actuator that is pneumatically actuated, delivering a realistic and effective haptic experience by simultaneously providing pressure, vibrotactile, and cold thermal feedback. The actuator features a design with multiple air chambers, each with controllable volume achieved through pneumatic valves connected to compressed air tanks. The lower air chamber generates pressure feedback, while the upper chamber produces vibrotactile feedback. In addition, two integrated lateral air nozzles create a cold thermal sensation. To showcase the system’s capabilities, we designed two unique 3D surfaces in the virtual environment: a frozen meat surface and an abrasive icy surface. These surfaces simulate tactile perceptions of coldness, pressure, and texture. Comprehensive performance assessments and user studies were conducted to validate the actuator’s effectiveness, highlighting its diverse feedback capabilities compared to traditional actuators that offer only single feedback modalities.

Index Terms—Multi-mode haptic feedback, silicone actuator, pneumatic, thermal feedback.

I. INTRODUCTION

VIRTUAL reality (VR) allows users to experience a life-like environment [1]. Most VR systems integrate software and hardware to simulate and generate appropriate visual and auditory signals [2]. There is an increasing demand for haptic feedback, as physical interaction is crucial in many VR applications. The absence of haptic feedback not only diminishes immersion but also significantly impacts the practicality of these applications [3]. Physical interaction encompasses various sensory signals such as pressure, vibration, movement, heat, force, and torque [4]. This paper specifically focuses on rendering tactile feedback.

Tactile signals are perceived through specialized sensory receptors known as thermoreceptors and mechanoreceptors located in the human skin [5]. These receptors are excited when appropriate external signals stimulate the skin. For instance, when a finger touches an object’s surface, the thermal energy stimulates the thermoreceptors, creating a thermal sensation.

This research was supported by the MSIT(Ministry of Science and ICT), Korea, in part under the Graduate School of Metaverse Convergence support program(IITP-2024-RS-2024-00425383) and in part under the ITRC(Information Technology Research Center) support program(IITP-2024-RS-2022-00156354), both supervised by the IITP(Institute for Information & Communications Technology Planning & Evaluation).

The authors are with the Kyunghee University College of Engineering, Computer Science & Engineering Yongin-si, Gyeonggi-do, South Korea (e-mail: ayon7019@gmail.com; ahsanraza@khu.ac.kr; sama.shoummo@gmail.com; jeon@khu.ac.kr (* Corresponding author)).

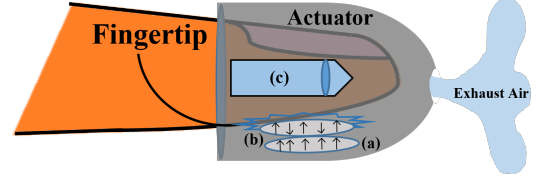


Fig. 1. Schematic diagram of the fingertip actuator. Air Chamber for (a) pressure feedback; (b)vibrotactile feedback; (c) nozzle for cold thermal feedback

At the same time, the shape of the surface deforms the skin, activating mechanoreceptors, and producing a sensation of pressure. Together, these sensations help us identify and further manipulate objects effectively.

High-fidelity physical interaction in virtual environments requires the simultaneous excitation of multiple tactile sensations, such as pressure, vibration, and temperature [6]. Thus, a comprehensive haptic system should provide multiple tactile sensations for a high-fidelity virtual experience. While conventional haptic systems typically rely on a single module for specific sensations, recent studies have explored incorporating multiple types of tactile feedback. To this end, a simple solution would be integrating multiple actuators into a system. For instance, Gallo et al. developed a flexible haptic interface capable of rendering both tactile and thermal stimuli using two actuators [7]. They proposed a hybrid electromagnetic-pneumatic system for tactile sensation and a Peltier module for thermal sensation. However, using multiple actuators often increases weight, which can limit usability, particularly when wearability is a priority.

A multi-mode haptic actuator presents a promising solution to the challenges mentioned earlier. Research has demonstrated that a pneumatically controlled soft actuator can deliver high-frequency vibrotactile feedback and pressure feedback using a single actuator [8], [9]. Additionally, it offers several functional advantages, including lightweight construction, flexibility, high strain density, and ease of fabrication to achieve the desired shape [10], [11]. Although the authors’ initial design provided only one type of feedback at a time with a single air bladder, they later expanded their work to develop a dual-layer pneumatic actuator capable of rendering both pressure and vibration feedback simultaneously [12].

Based on these works, the current paper proposes a multilayer silicone fingertip actuator that delivers cold thermal sensations and tactile sensations, such as pressure and vibration simultaneously, as shown in Figure 1. The actuator features two air chambers at the bottom and two lateral air nozzles along the inner-side walls. The bottom layers provide

pressure and vibration feedback by inflating and deflating the air chambers synchronously. Meanwhile, the lateral air nozzles produce cold thermal sensations using a vortex tube effect. A vortex tube is a mechanical device that separates compressed air into hot and cold streams through rapid spinning and centrifugal forces, creating a temperature gradient. Adjusting the air flow rate generates varying levels of cold sensation.

Following the introduction, the paper is organized as follows: Section II reviews the literature on multi-modal feedback systems. Section III details the actuator design and fabrication process. Section IV describes the system configuration. Section V presents the characterization and result of the actuator. Sections VI, VII, and VIII detail user perception evaluations. Finally, Section IX concludes the work.

II. RELATED WORK

This paper aims to deliver various types of tactile feedback along with thermal feedback. This section reviews existing methods for providing thermal feedback, followed by a survey of multi-mode haptic feedback that combines tactile and thermal sensations using multiple actuators in a single system.

A. Thermal Feedback Using Single Actuator

There are two ways of displaying thermal energy to human skin: contact-based (conduction) and non-contact-based (convection and radiation).

1) *Contact-based Thermal Feedback*: Thermal sensations are often experienced through conduction when touching an object. Many researchers have utilized Peltier modules to create thermal displays that convey temperature through conduction [13], [14]. These modules serve as temperature controllers, capable of both heating and cooling depending on the direction of the current. Some have integrated Peltier modules with head-mounted displays (HMDs) to provide thermal cues on the user's face. For example, Chen et al. developed a Peltier-based prototype integrated with the Oculus Rift HMD to deliver dynamic thermal sensations, simulating hot and cold wind [15], [16], and interacting with virtual kitchen equipment [17]. Peiris et al. created a thermal HMD system that provided directional thermal cues in VR games, exploring thermal feedback on the forehead for spatial localization tasks [18], [19]. They employed three Peltier modules to guide users toward target orientations through thermal haptic cues.

Wearable thermal modules have also been explored. Gallo et al. proposed a thermal display featuring four Peltier elements and copper diffusers for adjustable temperature feedback [20]. Garbardi et al. introduced a thermal display that combined two Peltier modules with a haptic thimble to provide transient heat in virtual environments [21]. Zhu et al. applied thermal feedback in a smart ring using thermoelectric coolers [22], while Peiris et al. developed the ThermalBracelet, which rendered spatial-temporal temperature feedback around the wrist using Peltier modules [23]. Kim et al. created untethered thermal gloves utilizing flexible thermoelectric devices for bidirectional heat stimuli [24], and Nijijima et al. presented the ThermalBitDisplay, which used tiny Peltier devices to deliver localized heat feedback [25].

Water has also been used to create thermal sensations. Hayakawa et al. developed a high-speed temperature display using water as a heat medium [26], while Günther et al. introduced a thermal display that provided on-body thermal feedback in VR using water at varying temperatures [27]. In addition, Peltier modules have also been employed for material recognition in several studies [5], [28].

2) *Non-Contact-based Thermal Feedback*: Recently, researchers have focused on developing advanced non-contact thermal display technology to simulate thermal sensations without physical contact. Nakajima et al. proposed a non-contact system that uses an ultrasound-phased array to direct cold air to a specific area on the user's skin [29]. Their solution comprises a storage unit for cold air that contains dry ice and a downward-firing tube to render the cold sensation. In another work, Xu et al. introduced a revolutionary non-contact cold thermal display that uses a vortex tube to render cold thermal feedback [30]. This device utilizes a developed cooling model that includes the velocity of the cold airflow and heat absorption from the skin. In another research, the author proposed a vortex-based approach to produce adjustable non-contact cold feelings [31]. By adjusting the distance and volume flow rate of the cold air, the device renders the sensations of various temperature perceptions. Recently, Makino et al. [32] proposed an experimental way to present the spatially continuous cold sensation based on low-temperature airflows. The author estimated the minimal distance at which two airflows were recognized as different cold stimuli, and the notion of a local cold stimulus group discrimination threshold (LCSGDT) was established. Satoshi et al. proposed a radiation-based thermal haptic display to render a hot sensation using a halogen lamp and mirror [33]. Wang et al. proposed an ultrasound-based heating circuit that delivers heated air to the user [34].

It is sometimes evidenced that providing thermal sensations alone does not significantly enhance realism; combining temperature feedback with other haptic sensations is crucial for achieving a high level of realism in the feeling of touch within a virtual environment. [6].

B. Thermal and Tactile Feedback Using Multiple Actuators

Many researchers have employed multiple actuators within a single haptic interface to deliver multi-mode thermal and tactile feedback. Guiatni et al. developed a haptic display that uses a Peltier pump integrated with mechanical linkages to provide thermal and other haptic feedback for minimally invasive surgery [35]. Gallo et al. proposed a haptic display incorporating Peltier-based hot and cold water chambers to render both temperature and pressure feedback [36]. Cai et al. introduced a pneumatic glove featuring an inflatable airbag and two temperature-controlled air chambers (hot and cold) that renders thermal and tactile feedback to simulate grasping objects of various temperatures and materials in a virtual environment [37].

Additionally, a fingertip-based haptic display was designed to simulate vertical and shearing forces, high-frequency tactile vibrations, and temperature feedback using motor pulleys,

belts, and a Peltier mechanism [38]. A hybrid feedback system was proposed to recreate tactile and thermal experiences in virtual environments using a fan, hot air blower, mist maker, and heat lamp [39]. Cho et al. introduced a data-driven haptic system that provides force, tactile, and temperature feedback using a vibration motor and a Peltier element attached to a force feedback device [40]. Oh et al. designed a multi-modal glove that offers vibration and temperature feedback using three vibrators and a heater sheet made from liquid metal eutectic gallium-indium [41]. Lee et al. proposed a haptic display that delivers tactile and thermal perception through internal balloon inflation systems and a heater sheet [42]. Furthermore, researchers also evaluated temperature pattern recognition while providing simultaneous vibrotactile feedback on the thenar eminence of the user's hand [43].

Combining multiple actuators to provide various haptic feedback modalities often leads to the common drawback of increased weight and complexity in the haptic system, which can diminish the overall quality of the haptic experience.

III. DESIGN AND FABRICATION

This section outlines the design and manufacturing process of our proposed actuator. In this paper, we focus specifically on integrating cold thermal feedback with pressure and vibration feedback. We designed a thimble-shaped end effector as the haptic interface, allowing it to effectively wrap around the fingertip without requiring additional attachments. This silicone-based actuator design also significantly enhances usability, as it is difficult to support heavy weight with the fingertip. Furthermore, the use of a flexible material improves wearability even more.

A. Multi-Modal Actuator Design Model

This section describes the design of our multi-modal thimble-shaped actuator, made from silicone, which simultaneously delivers sensations of cold temperatures, pressure, and vibrations. Figure 2 illustrates the schematic diagram of our proposed actuator. The actuator consists of two distinct air chambers and two lateral air nozzles, each serving a specific function to provide different types of feedback. The upper air chamber is designed for vibration feedback, while the lower chamber provides pressure feedback. The lateral air nozzles are dedicated to producing cold thermal feedback by circulating cold air. A small hole in front of the thimble directs the cold air outward, ensuring effective thermal feedback to the user.

The two air chambers are connected with a pair of pneumatic pipes to simulate pressure and vibration feedback. Positive and negative solenoid valves are attached to the pipes to control the inlet and exhaust of the airflow as shown in Figure 3.

Each lateral air nozzle is equipped with a pneumatic pipe connected to a vortex tube, which is in turn linked to an electrical variable pressure regulator, as illustrated in Figure 3. This configuration circulates cold air, enabling precise control over the air temperature.

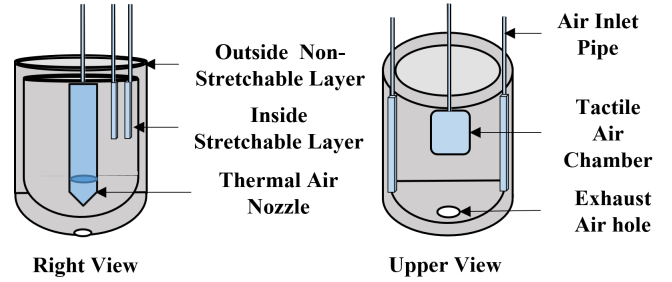


Fig. 2. The layout of the tactile air chambers and the nozzle for cold air in the actuator.

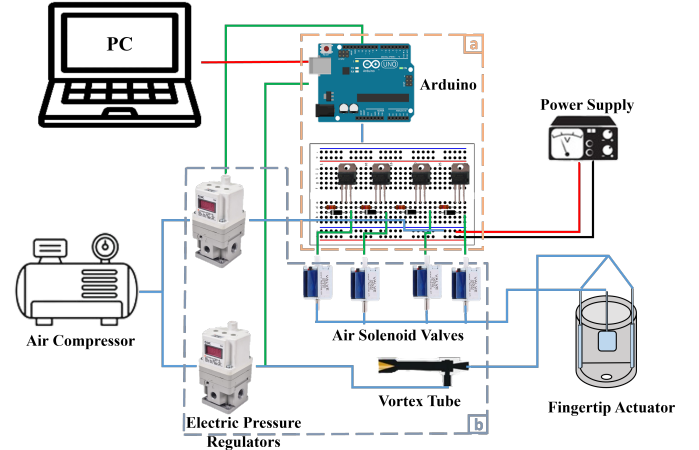


Fig. 3. Control system configuration. (a) Electronic control units; (b) pneumatic control units.

The outer wall of the actuator is made non-stretchable to maintain its structural integrity and original shape, while the inner wall is designed to be stretchable, allowing it to inflate against the user's skin for feedback. Dry polyester textiles are incorporated into the silicone molding process to create this non-stretchable layer.

The actuator is shaped like a thimble, with an average thickness that makes it easy to wear on the user's index finger. Although variations in fingertip sizes may affect the experiment's outcomes, it is feasible to manufacture new actuators in various sizes to accommodate users with different fingertip dimensions. Additionally, this actuator is flexible and lightweight, minimizing interference with normal hand movements.

B. Material Selection and Molding Process

Ecoflex 00-30 (Smooth-On, Inc., Macungie, PA, USA), with Young's modulus of 0.169 MPa, and a Shore hardness rating of 00-30, was selected for the construction of the actuator. This Ecoflex silicone provides 90% elongation at break and a 100% modulus of 10 psi, offering excellent flexibility and resilience [8]. These properties make it highly adaptable for the intended application.

The mold was made from acrylonitrile butadiene styrene (ABS) and designed to match the actuator's shape. The overall mold consisted of two parts: an inner mold to form the

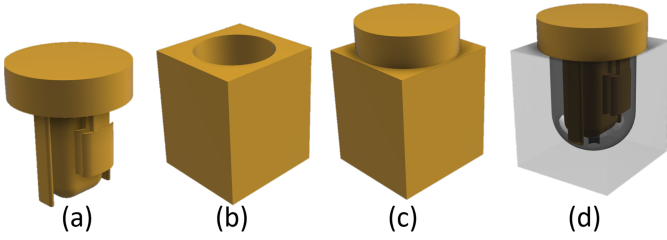


Fig. 4. Mold designs. (a) Internal mold; (b) External mold; (c) Combined (internal and external) mold structure; (d) Internal view of the combined mold structure

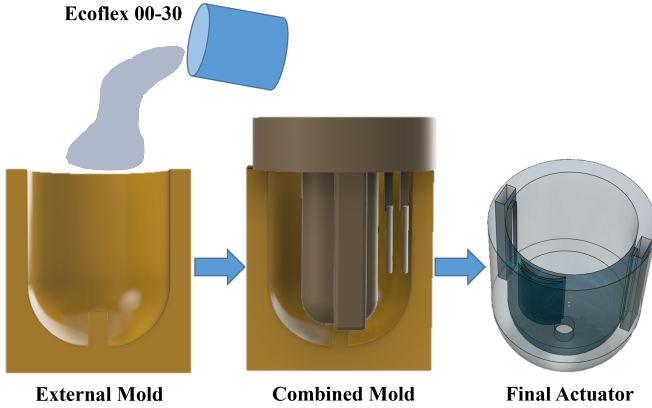


Fig. 5. Molding process to fabricate the actuator.

actuator's interior cavity and an outer mold to shape its external structure, as shown in Figure 4.

As shown in Figure 5, a simple molding process was required to develop the proposed actuator. Ecoflex 00-30 liquid was poured inside the mold. After pouring the liquid material, it needed to cure for a specific amount of time until it solidified.

IV. CONTROL MECHANISM

The main control mechanism is based on pneumatic actuation. This requires precise airflow regulation, including the directed circulation of cold air through the lateral air nozzles of the actuator. Additionally, it involves the systematic inflation and deflation of the actuator's two air chambers [9]. This systematic airflow regulation makes it possible to render thermal, pressure, and vibration feedback simultaneously.

Figure 3 illustrates the schematic diagram of our control mechanism, detailing all hardware components. There are two control systems: one for air temperature (connected to the vortex tube) and another for pressure and vibration (connected to the solenoid valves). First, the vortex tube utilizes airflow from an air source to manage the cold air temperature, separating compressed air into hot and cold streams through rapid spinning and centrifugal forces. An electric pressure regulator (SMC ITV3050) controls the airflow from the air source, which in turn regulates the cooling effect of the vortex tube by adjusting the flow rates.

Second, the amplitude of the pressure sensation and the frequency of the vibration sensation are adjusted by regulating

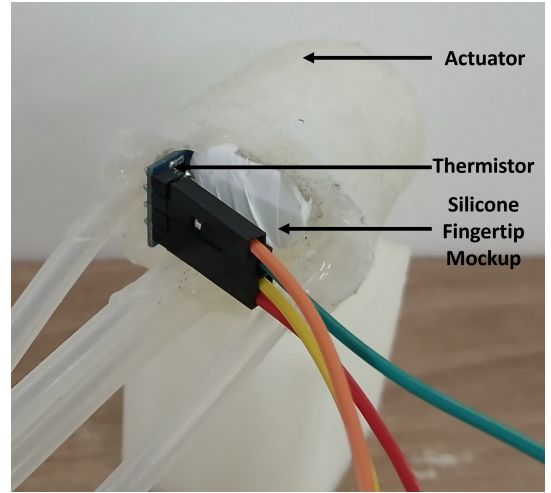


Fig. 6. Experimental setup for measuring temperature magnitude.

the inlet air in the air chambers. This system allows the actuator to provide responsive feedback by dynamically adjusting sensory stimuli. Four electrically controlled air solenoid valves (SC0526GC; Skoocom Technology Co. Ltd.) are used for this purpose: two valves facilitate airflow into the chambers, while the others enable air to be exhausted. Another electric pressure regulator (SMC ITV3050) controls the stiffness by managing the pressure within the air chambers.

An Arduino Uno microcontroller serves as the communication bridge between the computer and the actuator. Through the Arduino, digital and analog output commands from the computer are sent to the MOSFET transistor circuit, enabling serial communication. We included 1N4007 diodes in the circuit to ensure stable operation of the solenoid valves and to minimize transient voltage issues when the coils lose power. These commands control the operation of the air solenoid valves and the electric pressure regulators to produce various haptic feedback sensations.

A key design emphasis is on the simultaneous control of different feedback types. The control system is designed to allow independent and simultaneous management of both the regulators and valves. This allows for separate control of each component, facilitating the simultaneous delivery of different feedback signals when desired.

V. CHARACTERIZATION OF ACTUATOR

This section evaluates the actuator's characteristics. A series of measurements were taken, and the results were used to assess and render various types of haptic feedback. In all measurements, a silicone fingertip mock-up was inserted into the actuator to simulate a real finger. The performance of the pneumatic system relies on the actuator's material properties and the accuracy of the pneumatic valves.

A. Temperature Response for Thermal Feedback

First, we characterized the temperature control system of our proposed actuator.

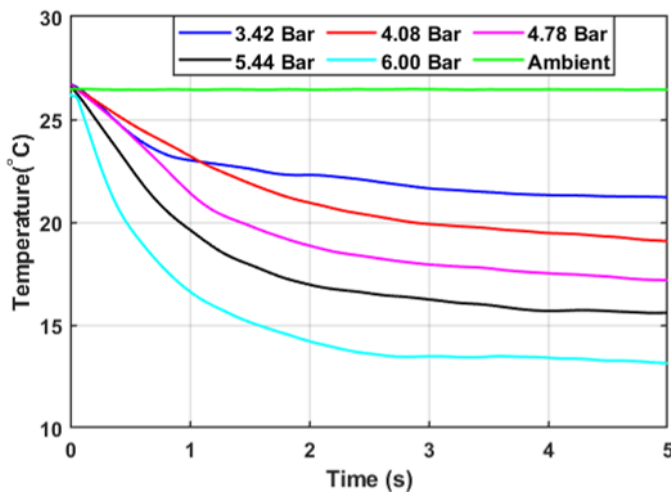


Fig. 7. Temperature changes with time for different air pressure levels.

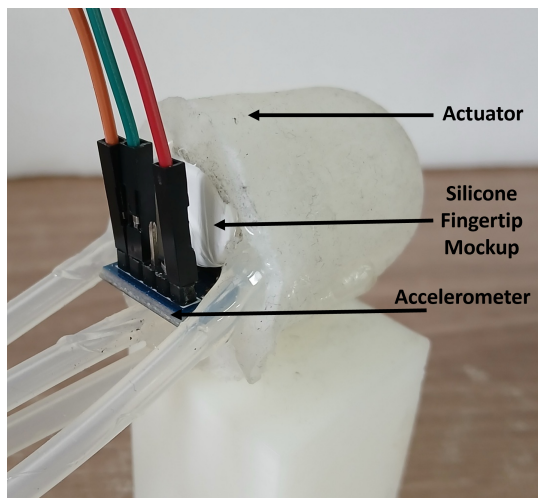


Fig. 8. Experimental setup for measuring vibration response.

1) *Measurement Setup and Procedure:* Figure 6 shows the experimental setup. A temperature sensor (MLX90614) was placed inside the actuator between the silicone fingertip mock-up and the cold air discharge point. Five air pressures, ranging from 3.42 to 6 bar, were used to generate varying temperatures with the Vortex tube. The flow rates of the input air ranged from $4.15 \text{ m}^3/\text{h}$ to $9.30 \text{ m}^3/\text{h}$.

2) *Result:* Figure 7 displays the temperature transitions observed at different pressure levels over a 5-second measurement period. The room temperature was maintained at 26°C throughout the experiment, providing a consistent baseline. The minimum temperature of the generated cold air was recorded at 13°C with an air pressure of 6.00 bar. Lower air pressure results in a smaller temperature drop. Additionally, the amount of temperature drop was found to be nearly linearly related to the air pressure level, enabling precise control of the temperature. In most cases, the temperature reached saturation after 2 seconds.

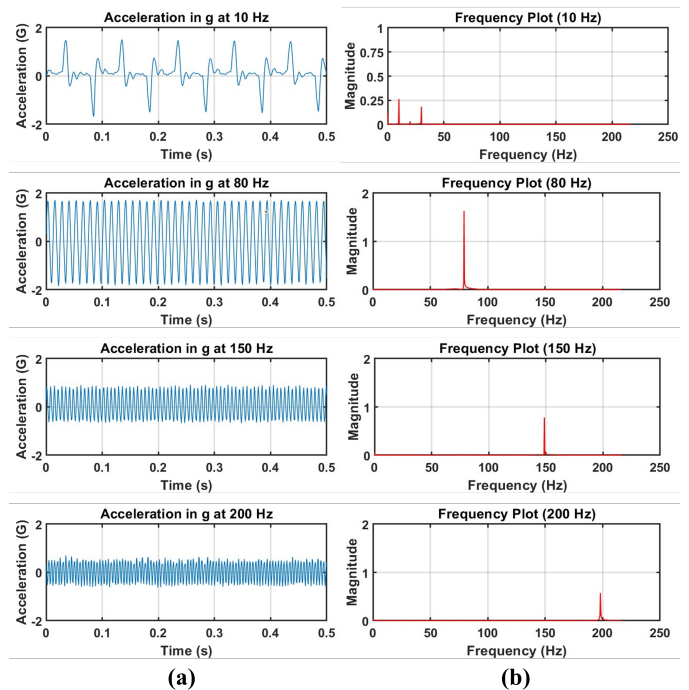


Fig. 9. Different acceleration spectrum for vibrotactile feedback in (a) time and (b) frequency domain.

B. Acceleration Response for Vibration Feedback

This experiment evaluates the frequency attributes of the actuator. This was essential to understand its performance and potential applications.

1) *Measurement Setup and Procedure:* Figure 8 illustrates our actual measurement setup. An accelerometer (GY-61) was mounted between the upper air chamber and the silicone fingertip mock-up. A data collection unit (NI-DAQ 6009) recorded the acceleration data, while MATLAB was used to store the data on the PC. The actuator's ability to provide vibrotactile feedback was evaluated across five frequencies, ranging from 10 Hz to 200 Hz. The accelerometer was calibrated prior to data collection, and with a sample rate of 1 kHz, acceleration measurements were recorded for 3 seconds at each frequency. A pressure regulator controlled the amplitude of each frequency at a pressure level of 5 psi.

2) *Result:* Figures 9(a), and 9(b) show vibration signals under various conditions in the time and frequency domains, respectively. The maximum amplitude was observed at 80 Hz, with an acceleration of 1.7 g. The amplitude noticeably decreases as the frequency approaches 200 Hz, peaking at a value of 0.6 g. Our actuator also shows a high acceleration amplitude at the lower end of the frequency spectrum, particularly at 1 Hz, in contrast to existing vibrotactile actuators.

C. Force Response for Pressure Feedback

This section characterized the pressure feedback of our proposed actuator.

1) *Measurement Setup and Procedure:* Figure 10 shows the measurement setup. A force sensor (Wenzhou SF20) was placed above the actuation chamber of the actuator. This sensor

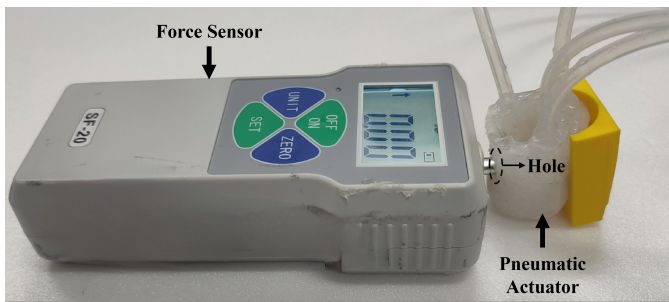


Fig. 10. Experimental setup for measuring pressure response.

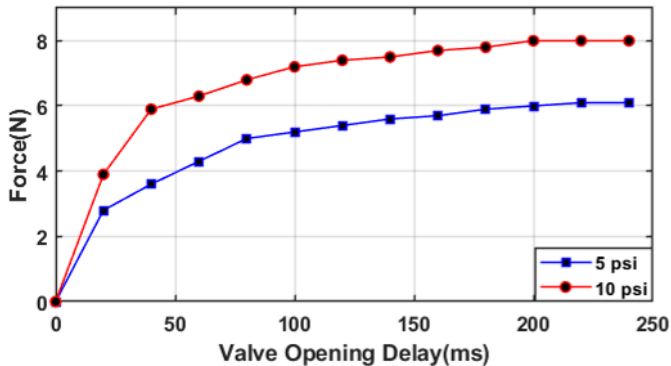


Fig. 11. Force measurement at different valve opening duration with two source pressure levels.

has a force-sensing resolution of 0.01N. Data was recorded at pressure levels of 5 psi and 10 psi by adjusting the pressure regulator. Each pressure level was measured by adjusting the duration of the solenoid valve opening in 20 ms increments, from 0 ms to 240 ms.

2) *Result:* Figure 11 illustrates the relationship between force magnitude and the valve opening duration. As expected, longer delays in the inlet pressure valve lead to greater force magnitudes. The trend peaks at 8 N with a valve opening delay of 200 ms at 10 psi, indicating that saturation occurs at this point. This behavior is attributed to the inherent pressure limitations of the pneumatic assembly when integrated with the end effector. Beyond the 8 N threshold, additional pressure primarily causes the flexible membrane to expand, increasing the contact area rather than the force. This effect persists up to 250 ms. It is important to note that keeping the solenoid valve open for more than 250 ms at 10 psi may damage the silicone air cell.

VI. USER STUDY 1: FREQUENCY DISCRIMINATION

We evaluated our system through three consecutive user studies. In the first evaluation, we focused on the actuator's capability as a vibration feedback transducer. For general vibration rendering, particularly in simulating roughness through vibrotactile signals, the most commonly used actuator is the voice-coil-type vibrator. We tested the perceptual performance of our actuator against one of the most advanced voice-coil vibrators on the market (Haptuator BM; Tactile Lab).

In this user study, we measured participants' ability to distinguish between different frequencies of vibration signals.

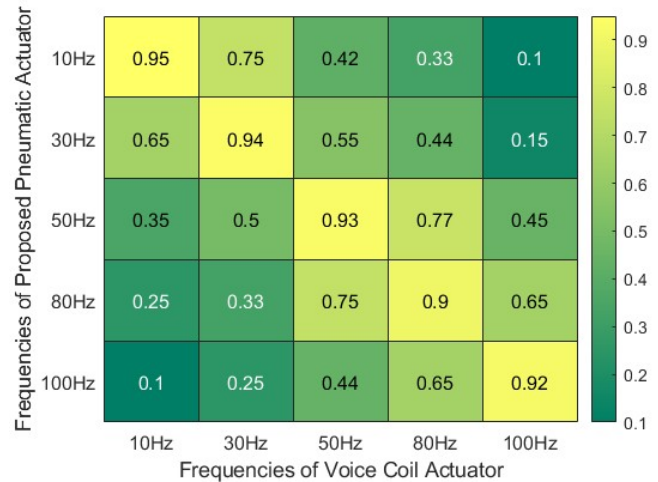


Fig. 12. Frequency similarity scores between the two actuators.

The vibration signals were generated by both the Haptuator and our actuator, and their discrimination performance was compared to validate the effectiveness of our actuator.

A. Participants

Fifteen participants (13 males, 2 females; average age 29) participated in the experiment. Seven had no experience with haptic rendering, while eight had general knowledge. None reported conditions affecting hand sensations. All participants gave their informed written consent to participate in this study. All experiments were approved by the Institutional Review Board (IRB) from the author's institution.

B. Stimuli and Experimental Design

The evaluation covers frequencies ranging from 10 Hz to 100 Hz. Five frequencies (10 Hz, 30 Hz, 50 Hz, 70 Hz, and 100 Hz) were rendered by the two actuators: our proposed pneumatic actuator and a voice coil-type actuator.

The vibration signals were delivered to the user's dominant thimble. A within-subject design was employed to test whether the vibrations produced by the two actuators were perceived similarly.

C. Experimental Procedure

Before the experiment, participants received detailed instructions, which they repeated to confirm their understanding. The experiment consisted of two stages: a training session and a main session. During the training session, participants experienced vibrotactile feedback at five different frequencies using a voice coil actuator.

In the main session, participants received pairwise vibrotactile feedback: a specific frequency from the voice coil actuator and five random frequencies from the pneumatic actuator. After each trial, participants rated the haptic similarity between the two stimuli on a scale from 0 to 1 (with 0 indicating completely different). This process created a similarity matrix. Each frequency pair was assessed for 10 seconds, with a

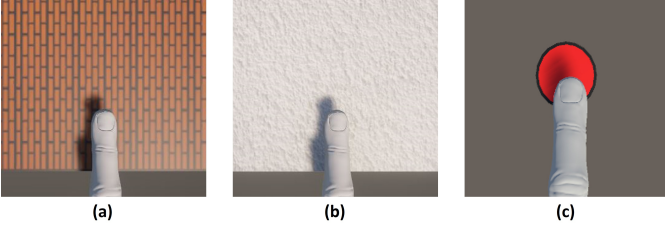


Fig. 13. (a) Grid Texture Surface, (b) Fine Texture Surface, and (c) 3D Button.

2-second interval between pairs. To minimize distractions, audio disturbances were eliminated during the main session, allowing participants to focus solely on the haptic feedback.

D. Result and Discussion

Figure 12 displays the mean similarity scores for all combinations. The vertical axis represents the rendered frequencies using our actuator, while the horizontal axis indicates those rendered by the voice coil actuator. The mean similarity score for the correctly matched pairs (diagonal blocks) is 0.93.

These results suggest that the quality of frequency rendering by our actuator is comparable to that of the advanced voice coil actuator across the entire frequency range.

VII. USER STUDY 2: EFFECT OF MULTI-MODAL FEEDBACK ON REALISM

The second experiment evaluated how multiple simultaneous feedback types enhance haptic realism. Three simple interaction scenarios were implemented: stroking two different textured surfaces (see Figures 13(a) and 13(b)) and pressing a push button (see Figure 13(c)).

Two conditions were compared: one that utilized our multi-mode actuator to create the sensation of surface and texture through pressure and vibration and another that employed a conventional single voice-coil actuator, which provided only vibration feedback. By comparing the perceived realism between these two conditions, we aimed to investigate the impact of the additional pressure feedback on user-perceived realism.

A. Stimuli

The two virtual textured surfaces and the virtual push button were presented to the participants. For texture rendering, separate algorithms were required for the two actuators due to their distinct specifications and control schemes. During the interaction, the user's fingertip position was tracked using an external optical tracker [44].

For our pneumatic actuator, a quasi-static pressure is first rendered during a contact. Simultaneously, roughness is simulated by high-frequency vibration. However, for this actuator, it is not quite possible to control the accelerations based on an arbitrary acceleration profile since the vibration is controlled by discretely opening or closing the valves for the air chamber. To address this, we employed a grid-based algorithm. Virtual grids are defined on the surface, and a short vibration burst is triggered as the user's finger passes over each grid. The spatial frequency of the grid and the vibration amplitude determine

the perceived roughness of the texture, with coarse and fine textures differing in grid frequency.

In comparison, the voice-coil actuator is more flexible in control as it gets an arbitrarily shaped waveform and produces a similar acceleration pattern. For a fair comparison, we adapted a state-of-the-art texture rendering algorithm from previous studies [45]–[48] to our setup. This algorithm generates a noisy vibration pattern while the user strokes the surface. It dynamically adjusts the vibration pattern based on the user's stroking velocity, with frequency and amplitude decreasing as velocity decreases. The roughness of the surface is determined by the frequency and amplitude of the underlying noise pattern. It is important to note that the voice-coil actuator does not provide static pressure for the sensation of contact.

The final scenario involves a virtual push button. The button is designed to trigger a virtual haptic click feedback at a specific height. When the user's finger reaches this height, a short step acceleration is produced to mimic the impact of clicking. This step acceleration is generated by quickly opening the positive valve for the pneumatic actuator or sending a step command signal for the voice-coil actuator.

B. Participants and Experimental Design

These experiments had the same participants as User Study 1. All participants gave their informed written consent to participate in this study. All experiments were approved by the Institutional Review Board (IRB) from the author's institution. A within-subject design was employed for the study. For each participant, the exploration on the surfaces using the two systems was repeated twice, yielding 8 explorations per participant. They were also asked to push the virtual 3D button using the same two actuators. Pushing the 3D button using both actuators was repeated five times, yielding 10 explorations per participant.

C. Experimental Procedure

Before starting the experiment, the participants were instructed about the procedure. We confirmed that participants correctly understood the procedure by asking them to repeat the instructions. This experiment was divided into training and main sessions.

In the training session, participants were introduced to the two types of actuators and the virtual environments. During the main session, participants were sound-blocked while they explored the virtual 3D surfaces and the virtual button using both actuators. The order of presentation was randomized. After exploring the surfaces and the button, participants were asked to rate the overall feedback fidelity by providing scores to the operator in response to the following questions: a) How realistic was the feedback? (realism), b) Was the feedback unnatural? (reverse scale), and c) How responsive was the feedback to actions in the VR environment? Ratings were given on a scale from 0 to 100 (0 meaning "Not at all" and 100 meaning "Very much"). The entire experiment took approximately thirty minutes to complete for each participant.

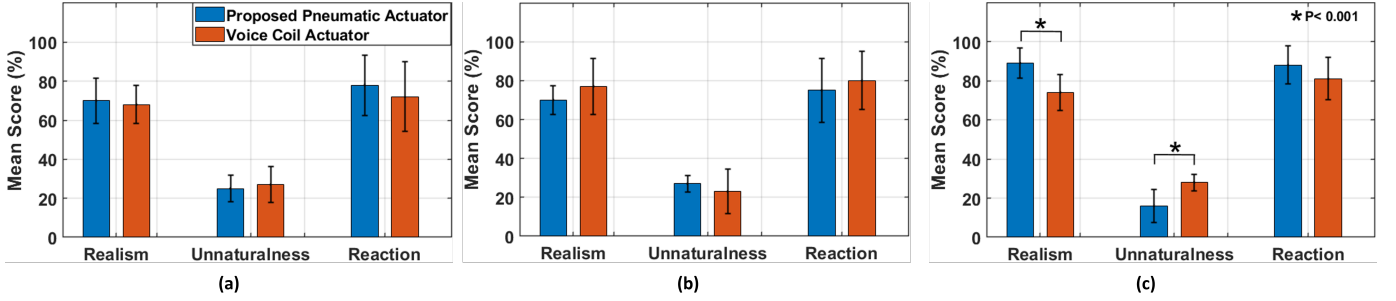


Fig. 14. Performance comparison between the proposed pneumatic and the voice coil actuator under three conditions; (a) coarse texture surface, (b) fine texture surface, and (c) 3D button.

D. Result and Discussion

Figures 14 present the average scores and standard errors for the two different textured surfaces and the 3D button. To analyze the data statistically, we conducted a one-way ANOVA with repeated measures. Post hoc comparisons using the Tukey test revealed no significant differences ($p > 0.05$) between the proposed pneumatic actuator and the voice coil actuator for the coarse textured surface (Figure 14(a)) and the fine-textured surface (Figure 14(b)). However, for the 3D button, participants preferred the pneumatic actuator over the voice coil actuator based on measures of realism and unnaturalness, showing a significant difference ($p < 0.001$) between the two actuators.

For the texture scenarios, no significant realism difference was observed. We speculate that although the pneumatic actuator uses a less sophisticated rendering algorithm compared to the state-of-the-art algorithm for the voice-coil, it still preserves the comparable realism due to the additional cue provided by static pressure for contact. However, further investigation is required to pinpoint the causes. Additionally, we noted that the voice coil actuator performed slightly better on the fine rough surface (Figure 14(b)), likely due to its superior high-frequency rendering capability.

For the 3D button, the pneumatic actuator was favored for the 3D button interaction. We believe this preference arises because rendering a virtual push button does not require a complex acceleration pattern. Thus, while both actuators provide high-quality feedback in terms of high-frequency vibration, the score difference can be attributed to the pneumatic actuator's ability to render quasi-static pressure for a more realistic contact feeling.

VIII. USER STUDY 3: OVERALL REALISM ASSESSMENT

The third experiment compares combined thermo-tactile feedback with single modalities to assess its impact on virtual reality applications. We designed two VR scenarios that integrate haptic feedback conditions with immersive visual stimuli.

A. VR Environments

To demonstrate the effectiveness of the proposed multi-mode actuator, we implemented two VR application scenarios. The first scenario involves touching a frozen meat surface,

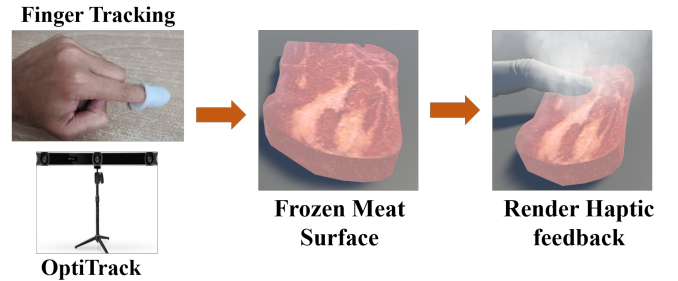


Fig. 15. System for rendering frozen meat surface.

allowing participants to experience simultaneous sensations of contact pressure, cold thermal feedback, and surface stiffness. The second scenario features interaction with an abrasive icy surface, enabling the perception of contact pressure, cold thermal feedback, and surface texture. The virtual environments were developed using the Unity game engine (version 2020.3.43f1). The user's finger was tracked using an optical tracker (OptiTrack Trio, V120, NaturalPoint, Inc., Corvallis, OR, USA) [44], and the tracked finger was visually represented in the scenes.

1) *Touching Frozen Meat Surface: simultaneous cold, pressure, and stiffness feedback:* This scenario enables participants to perceive contact pressure, cold thermal feedback, and surface stiffness while interacting with a frozen meat surface. This section outlines the control schemes and rendering algorithms used to deliver these three simultaneous feedback modalities.

Figure 15 illustrates the rendering hardware and the virtual scene. When the user makes contact with the surface, both contact pressure and thermal feedback are activated, simulating the sensation of touching a cold surface. Simultaneously, dynamic pressure is applied in response to the user pressing on the frozen meat, creating a realistic perception of stiffness.

The entire rendering algorithm is detailed in Algorithm 1. The function *isTouched* checks if the virtual representation of the user's finger, P , is in contact with a specific mesh, $MeatMesh$, within a 3D virtual environment. Here, $MeatMesh$ represents the surface of frozen meat. The constant pressure level intended to simulate contact is denoted by cp and is set at 3N. The indentation d is calculated based on the difference between the current position of the finger P and its initial position $P_{initial}$. The target stiffness coefficient, k , is retrieved

Algorithm 1 Frozen Meat Surface Rendering Process

```

1: Input: User finger position ( $P$ )
2: while isTouched( $P, MeatMesh$ ) do
3:    $cp \leftarrow 3N$  {Constant pressure level for contact feeling}

4:    $d \leftarrow |P - P_{initial}|$  {indentation calculation}
5:    $k \leftarrow \text{getTargetStiffness}(MeatMesh)$  {Retrieve target stiffness}
6:   RenderPressure( $cp + (kd)$ ) {Render pressure for both contact and stiffness feeling}
7:    $T \leftarrow \text{getTargetTemperature}(MeatMesh)$  {Retrieve target temperature}
8:   RenderThermal( $T$ ) {Render cold temperature sensation}
9: end while
10:
11: Finish
  
```



Fig. 16. System for rendering abrasive icy surface.

from the properties of *Mesh*. The function *RenderPressure*($cp + k(d)$) is used to render the sensation of pressure, combining both contact cp and stiffness feedback (the product of k and d). The target temperature T is also retrieved from the properties of *Mesh*, and the function *RenderThermal*(T) is used to render a cold temperature sensation, where T specifies the temperature to be simulated.

2) *Touching Abrasive Icy Surface: Simultaneous Cold Thermal, Contact Pressure, and Texture Feedback:* This scenario is designed to allow the user to perceive contact pressure, cold thermal feedback, and the texture of surface roughness while stroking across the surface. Figure 16 displays the setup and the VR scene. For texture rendering, the grid-based algorithm introduced VII is utilized.

The rendering algorithm in Algorithm 2 closely resembles that of Algorithm 1, with the primary distinction being in the vibration generation for texture feedback (lines 6-9). The texture rendering part first retrieves the grid structure from the contacting mesh and checks if the user’s hand is passing over one of the grids. If so, it generates short vibration bursts to simulate the acceleration associated with surface roughness. The faster the user’s movement, the stronger the vibration experienced.

B. Participants

A subset of ten participants (8 males, 2 females; average age 29) from the previous experiment participated in this

Algorithm 2 Abrasive Icy Surface Rendering Process

```

1: Input: User finger position ( $P$ )
2: while isTouched( $P, IcyMesh$ ) do
3:    $cp \leftarrow 3N$  {Constant pressure level for contact feeling}

4:   RenderPressure( $cp$ ) {Render constant pressure for contact feeling}
5:    $G \leftarrow \text{getTargetTextureGrid}(IcyMesh)$  {Retrieve the texture grid structure of the target surface}
6:   if isPassingGrid( $P, G$ ) then
7:      $V \leftarrow \text{getVelocity}()$  {Retrieve the velocity of the finger}
8:     RenderVibrationFeedback( $V$ ) {Render velocity-dependent tick vibration}
9:   end if
10:   $T \leftarrow \text{getTargetTemperature}(IcyMesh)$  {Retrieve target temperature}
11:  RenderThermal( $T$ ) {Render cold temperature sensation}
12: end while
13:
14: Finish
  
```

user study. Seven had no experience with haptic rendering, and three had general knowledge. None reported conditions affecting hand sensations. All participants gave their informed written consent to participate in this study. All experiments were approved by the Institutional Review Board (IRB) from the author’s institution.

C. Experimental Design

Four haptic feedback conditions were the subject of a within-subject experiment: a) *No feedback (NF)*, b) *Tactile feedback (TF)*, c) *Cold thermal feedback (CTF)*, and d) *Simultaneous thermal-tactile feedback (STF)*. *No feedback* refers to a condition in which there was neither cold thermal feedback nor tactile haptic feedback. *Tactile feedback* presented stiffness plus contact pressure feedback for the cold meat surface, and texture plus contact pressure feedback for the abrasive icy surface, without activating the cold thermal feedback. *Cold thermal feedback* presented just cold thermal feedback, with no tactile feedback. Finally, *Simultaneous thermal-tactile feedback* offered both tactile and cold thermal feedback simultaneously.

To assess participants’ experiences, we developed questionnaire sheets that included five measures:

- 1) Realism – The feedback felt realistic and akin to real-world tactile sensations.
- 2) Localization – The precise location of the haptic feedback was identifiable within the VR environment.
- 3) Tactility – The quality of the tactile feedback was perceived as very high.
- 4) Reaction – The system synchronized effectively with user interactions in the VR setting.
- 5) Immersion – The haptic feedback contributed to maintaining interest in the VR world.

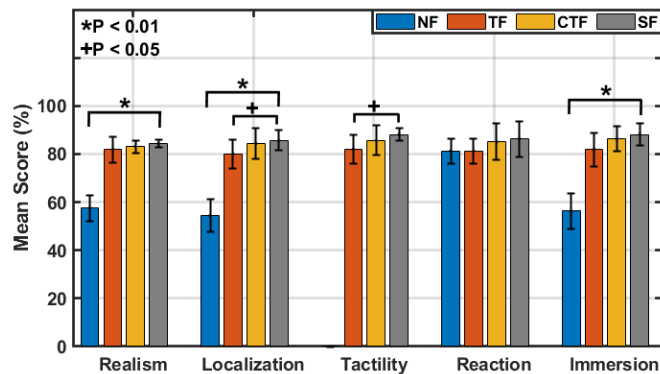


Fig. 17. Mean scores and standard error of all the measures in different feedback conditions for frozen meat surface.

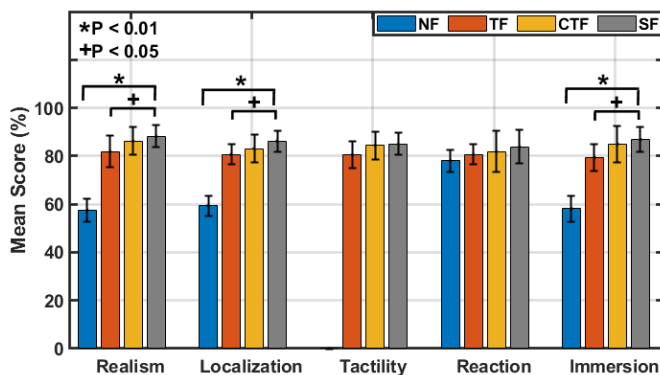


Fig. 18. Mean scores and standard error of all the measures in different feedback conditions for abrasive icy surface

After each condition, participants rated each question on a continuous scale from 0 to 100, with "Not at all" and "Very much" as the endpoints for each feedback condition.

D. Experimental Procedure

Before the experiment began, we provided participants with detailed instructions and confirmed their understanding by having them repeat the guidelines. The experiment consisted of a training session followed by a main session. During the training session, participants experienced the four unique feedback modes. In the main session, they interacted with each surface type twice while employing all four feedback conditions. After each scene, participants completed the questionnaire. There was a 5-minute interval between the two scenes. Overall, the experiment lasted approximately fifteen minutes for each participant, and audio distractions were minimized throughout the main session to ensure focus on the haptic feedback.

E. Result and Discussion

Figures 17 and 18 illustrate the average scores and standard errors for the frozen meat surface and abrasive icy surface scenarios respectively.

A one-way ANOVA with repeated measurements was used to analyze the collected data. Post hoc comparison using the Tukey test revealed a significant difference ($p < 0.01$)

between *Simultaneous cold thermal-tactile feedback* and *No feedback* for the first, second, and fifth measures in both scenarios. Furthermore, a significant difference was observed between *Tactile feedback* and *Simultaneous thermal-tactile feedback* for the second and third measures ($p < 0.05$) on the meat surface scenario, while for the first, second, and fifth measures on the abrasive icy surface scenario. However, no significant difference was found between *Tactile feedback* and *Cold thermal feedback* across any measures in either scenario. Moreover, Users rated the third measure in the *No feedback* condition as zero due to the lack of tactility in both scenarios.

The results indicate that integrating tactile and cold thermal cues can significantly enhance the virtual experience. In both VR environments, *Simultaneous thermal-tactile feedback* was the preferred choice across all measures. Conversely, *no feedback* was consistently rated the least favorably, while all other feedback conditions were preferred over this baseline. Overall, our multi-modal approach proves beneficial in increasing haptic realism in suitable interaction scenarios.

IX. CONCLUSION

This work introduces a silicone-based fingertip actuator designed to replicate realistic tactile sensations by delivering multiple types of haptic feedback. The actuator simultaneously provides thermal, pressure, and vibrotactile feedback through dual air chambers and lateral air nozzles. This design enables users to experience subtle temperature variations and tactile sensations (pressure and vibration) that closely mimic real-world interactions.

The actuator is adaptable, accommodating various finger sizes and featuring adjustable air chambers to control feedback intensity. Additionally, pressure modulation based on depth enhances realism during interactions with virtual surfaces, as demonstrated in successful tests on cold meat surfaces.

This approach serves as an effective alternative to conventional wearable haptic devices, which often struggle to provide comprehensive multi-modal feedback using a single actuator. Its potential applications span education, safety training, medical training, and rehabilitation, enriching the realism of virtual training experiences. The actuator enhances haptic technology with its flexible and efficient design, ultimately improving user experiences and contributing to advancements in virtual and augmented reality systems.

REFERENCES

- [1] Pietro Cipresso, Irene Alice Chicchi Giglioli, Mariano Alcañiz Raya, and Giuseppe Riva. The past, present, and future of virtual and augmented reality research: a network and cluster analysis of the literature. *Frontiers in psychology*, 9:309500, 2018.
- [2] Sara Price, Carey Jewitt, and Nikoleta Yiannoutsou. Conceptualising touch in vr. *Virtual Reality*, 25(3):863–877, 2021.
- [3] RK Venkatesan, Domna Banakou, and Mel Slater. Haptic feedback in a virtual crowd scenario improves the emotional response. *Frontiers in Virtual Reality*, 4:1242587, 2023.
- [4] Heather Culbertson, Samuel B Schorr, and Allison M Okamura. Haptics: The present and future of artificial touch sensation. *Annual Review of Control, Robotics, and Autonomous Systems*, 1:385–409, 2018.
- [5] Hsin-Ni Ho. Material recognition based on thermal cues: Mechanisms and applications. *Temperature*, 5(1):36–55, 2018.

- [6] Mingyu Kang, Cheol-Gu Gang, Sang-Kyu Ryu, Hyeon-Ju Kim, Da-Yeon Jeon, and Soonjae Pyo. Haptic interface with multimodal tactile sensing and feedback for human-robot interaction. *Micro and Nano Systems Letters*, 12(1):9, 2024.
- [7] Simon Gallo, Choonghyun Son, Hyunjoo Jenny Lee, Hannes Bleuler, and Il-Joo Cho. A flexible multimodal tactile display for delivering shape and material information. *Sensors and Actuators A: Physical*, 236:180–189, 2015.
- [8] Aishwari Talhan, Hwangil Kim, and Seokhee Jeon. Tactile ring: Multi-mode finger-worn soft actuator for rich haptic feedback. *IEEE Access*, 8:957–966, 2019.
- [9] Ahsan Raza, Waseem Hassan, and Seokhee Jeon. Pneumatically controlled wearable tactile actuator for multi-modal haptic feedback. *IEEE Access*, 2024.
- [10] Daisuke Sasaki, Toshiro Noritsugu, and Masahiro Takaiwa. Development of active support splint driven by pneumatic soft actuator (assist). In *Proceedings of the 2005 IEEE international conference on robotics and automation*, pages 520–525. IEEE, 2005.
- [11] Aslan Miriyev, Kenneth Stack, and Hod Lipson. Soft material for soft actuators. *Nature communications*, 8(1):596, 2017.
- [12] Mohammad Shadman Hashem, Joolekha Bibi Joolee, Waseem Hassan, and Seokhee Jeon. Soft pneumatic fingertip actuator incorporating a dual air chamber to generate multi-mode simultaneous tactile feedback. *Applied Sciences*, 12(1):175, 2021.
- [13] Barbara Deml, Andreas Mihalyi, and Gunter Hannig. Development and experimental evaluation of a thermal display. In *Proc. EuroHaptics Conf*, pages 257–262. Citeseer, 2006.
- [14] Hidetaka Morimitsu and Seichiro Katsura. Thermal bilateral control with scaled thermal information using peltier device. In *2011 IEEE/SICE International Symposium on System Integration (SII)*, pages 521–526. IEEE, 2011.
- [15] Zikun Chen, Roshan Lalintha Peiris, and Kouta Minamizawa. A thermal pattern design for providing dynamic thermal feedback on the face with head mounted displays. In *Proceedings of the Eleventh International Conference on Tangible, Embedded, and Embodied Interaction*, pages 381–388, 2017.
- [16] Zikun Chen, Roshan Lalintha Peiris, and Kouta Minamizawa. A thermally enhanced weather checking system in vr. In *Adjunct Proceedings of the 30th Annual ACM Symposium on User Interface Software and Technology*, pages 123–125, 2017.
- [17] Zikun Chen, Wei Peng, Roshan Peiris, and Kouta Minamizawa. Thermo-reality: Thermally enriched head mounted displays for virtual reality. In *ACM SIGGRAPH 2017 Posters*, pages 1–2. ACM Digital Library, 2017.
- [18] Roshan Lalintha Peiris, Wei Peng, Zikun Chen, Liwei Chan, and Kouta Minamizawa. Thermovr: Exploring integrated thermal haptic feedback with head mounted displays. In *Proceedings of the 2017 CHI Conference on Human Factors in Computing Systems*, pages 5452–5456, 2017.
- [19] Roshan Lalintha Peiris, Wei Peng, Zikun Chen, and Kouta Minamizawa. Exploration of cuing methods for localization of spatial cues using thermal haptic feedback on the forehead. In *2017 IEEE World Haptics Conference (WHC)*, pages 400–405. IEEE, 2017.
- [20] Simon Gallo, Giulio Rognini, Laura Santos-Carreras, Tristan Vouga, Olaf Blanke, and Hannes Bleuler. Encoded and crossmodal thermal stimulation through a fingertip-sized haptic display. *Frontiers in Robotics and AI*, 2:25, 2015.
- [21] Massimiliano Gabardi, Daniele Leonardis, Massimiliano Solazzi, and Antonio Frisoli. Development of a miniaturized thermal module designed for integration in a wearable haptic device. In *2018 IEEE Haptics Symposium (HAPTICS)*, pages 100–105. IEEE, 2018.
- [22] Kening Zhu, Simon Perrault, Taizhou Chen, Shaoyu Cai, and Roshan Lalintha Peiris. A sense of ice and fire: Exploring thermal feedback with multiple thermoelectric-cooling elements on a smart ring. *International Journal of Human-Computer Studies*, 130:234–247, 2019.
- [23] Roshan Lalitha Peiris, Yuan-Ling Feng, Liwei Chan, and Kouta Minamizawa. Thermalbracelet: Exploring thermal haptic feedback around the wrist. In *Proceedings of the 2019 CHI Conference on Human Factors in Computing Systems*, pages 1–11, 2019.
- [24] Seung-Won Kim, Sung Hee Kim, Choong Sun Kim, Kyoungsoo Yi, Jun-Sik Kim, Byung Jin Cho, and Youngsu Cha. Thermal display glove for interacting with virtual reality. *Scientific reports*, 10(1):11403, 2020.
- [25] Arinobu Nijijima, Toki Takeda, Takafumi Mukouchi, and Takashi Satou. Thermalbitdisplay: Haptic display providing thermal feedback perceived differently depending on body parts. In *Extended Abstracts of the 2020 CHI Conference on Human Factors in Computing Systems*, pages 1–8, 2020.
- [26] Kyohei Hayakawa, Kazuki Imai, Ryo Honaga, and Masamichi Sakaguchi. High-speed thermal display system that synchronized with the image using water flow. *Haptic Interaction: Perception, Devices and Applications*, pages 69–74, 2015.
- [27] Sebastian Günther, Florian Müller, Dominik Schön, Omar Elmoghazy, Max Mühlhäuser, and Martin Schmitz. Terminator: Understanding the interdependency of visual and on-body thermal feedback in virtual reality. In *Proceedings of the 2020 CHI Conference on Human Factors in Computing Systems*, pages 1–14, 2020.
- [28] Hyejin Choi, Seongwon Cho, Sunghwan Shin, Hojin Lee, and Seungmoon Choi. Data-driven thermal rendering: An initial study. In *2018 IEEE Haptics Symposium (HAPTICS)*, pages 344–350. IEEE, 2018.
- [29] Mitsuru Nakajima, Keisuke Hasegawa, Yasutoshi Makino, and Hiroyuki Shinoda. Remotely displaying cooling sensation via ultrasound-driven air flow. In *2018 IEEE Haptics Symposium (HAPTICS)*, pages 340–343. IEEE, 2018.
- [30] Jiayi Xu, Yoshihiro Kuroda, Shunsuke Yoshimoto, and Osamu Oshiro. Non-contact cold thermal display by controlling low-temperature air flow generated with vortex tube. In *2019 IEEE World Haptics Conference (WHC)*, pages 133–138. IEEE, 2019.
- [31] Jiayi Xu, Shunsuke Yoshimoto, Naoto Ienaga, and Yoshihiro Kuroda. Intensity-adjustable non-contact cold sensation presentation based on the vortex effect. *IEEE Transactions on Haptics*, 15(3):592–602, 2022.
- [32] Koyo Makino, Jiayi Xu, Akiko Kaneko, Naoto Ienaga, and Yoshihiro Kuroda. Spatially continuous non-contact cold sensation presentation based on low-temperature airflows. In *2023 IEEE World Haptics Conference (WHC)*, pages 223–229. IEEE, 2023.
- [33] Satoshi Saga. Heathapt thermal radiation-based haptic display. *Haptic Interaction: Perception, Devices and Applications*, pages 105–107, 2015.
- [34] Yida Wang and Yi-Chao Chen. Non-contact thermal haptics for vr. In *Adjunct Proceedings of the 2023 ACM International Joint Conference on Pervasive and Ubiquitous Computing & the 2023 ACM International Symposium on Wearable Computing*, pages 386–390, 2023.
- [35] Mohamed Guiatni, Vincent Riboulet, Christian Duriez, Abderrahmane Kheddar, and Stéphane Cotin. A combined force and thermal feedback interface for minimally invasive procedures simulation. *Ieee/Asme Transactions On Mechatronics*, 18(3):1170–1181, 2012.
- [36] Simon Gallo, Lucian Cucu, Nicolas Thevenaz, Ali Sengül, and Hannes Bleuler. Design and control of a novel thermo-tactile multimodal display. In *2014 IEEE Haptics Symposium (Haptics)*, pages 75–81. Ieee, 2014.
- [37] Shaoyu Cai, Pingchuan Ke, Takuji Narumi, and Kening Zhu. Thermo-glove: A pneumatic glove for thermal perception and material identification in virtual reality. In *2020 IEEE conference on virtual reality and 3D user interfaces (VR)*, pages 248–257. IEEE, 2020.
- [38] Takaki Murakami, Tanner Person, Charith Lasantha Fernando, and Kouta Minamizawa. Altered touch: miniature haptic display with force, thermal and tactile feedback for augmented haptics. In *ACM SIGGRAPH 2017 Posters*, pages 1–2. ACM Digital Library, 2017.
- [39] Ping-Hsuan Han, Yang-Sheng Chen, Kong-Chang Lee, Hao-Cheng Wang, Chiao-En Hsieh, Jui-Chun Hsiao, Chien-Hsing Chou, and Yi-Ping Hung. Haptic around: multiple tactile sensations for immersive environment and interaction in virtual reality. In *Proceedings of the 24th ACM symposium on virtual reality software and technology*, pages 1–10, 2018.
- [40] Seongwon Cho, Hyejin Choi, Sunghwan Shin, and Seungmoon Choi. Data-driven multi-modal haptic rendering combining force, tactile, and thermal feedback. In *Haptic Interaction: Perception, Devices and Algorithms 3*, pages 69–74. Springer, 2019.
- [41] Jinhyeok Oh, Suin Kim, Sangyeop Lee, Seongmin Jeong, Seung Hwan Ko, and Joobum Bae. A liquid metal based multimodal sensor and haptic feedback device for thermal and tactile sensation generation in virtual reality. *Advanced Functional Materials*, 31(39):2007772, 2021.
- [42] Eun-Hyuk Lee, Sang-Hoon Kim, and Kwang-Seok Yun. Three-axis pneumatic haptic display for the mechanical and thermal stimulation of a human finger pad. In *Actuators*, volume 10, page 60. MDPI, 2021.
- [43] Anshul Singhal and Lynette A Jones. Perceptual interactions in thermo-tactile displays. In *2017 IEEE World Haptics Conference (WHC)*, pages 90–95. IEEE, 2017.
- [44] Optitrack. Optitrack v120: Trio. <https://optitrack.com/products/v120-trio/>, 2018. Available online; accessed 5 September 2018.
- [45] Heather Culbertson, Juliette Unwin, and Katherine J Kuchenbecker. Modeling and rendering realistic textures from unconstrained tool-surface interactions. *IEEE transactions on haptics*, 7(3):381–393, 2014.
- [46] Arsen Abdulali and Seokhee Jeon. Data-driven rendering of anisotropic haptic textures. In *Haptic Interaction: Science, Engineering and Design 2*, pages 401–407. Springer, 2018.
- [47] Weizhi Nai, Jianyu Liu, Chongyang Sun, Qinglong Wang, Guohong Liu, and Xiaoying Sun. Vibrotactile feedback rendering of patterned textures

using a waveform segment table method. *IEEE Transactions on Haptics*, 14(4):849–861, 2021.

- [48] Negin Heravi, Heather Culbertson, Allison M Okamura, and Jeannette Bohg. Development and evaluation of a learning-based model for real-time haptic texture rendering. *IEEE Transactions on Haptics*, 2024.